Theor Chem Acc (2011) 129:527–543
DOI 10.1007/s00214-011-0893-0

REGULAR ARTICLE

Quantitative vibronic coupling calculations: the formyloxyl radical

Kerstin Klein · Etienne Garand · Takatoshi Ichino · Daniel M. Neumark · Jürgen Gauss · John F. Stanton

Received: 22 November 2010 / Accepted: 11 January 2011 / Published online: 5 February 2011

Abstract The performance of different choices of parametrization for the quasidiabatic Hamiltonian approach of Köppel et al. (Adv Chem Phys 57:59, 1984) is studied for the $\tilde{X}^2A_1$ and $\tilde{A}^2B_2$ states of the formyloxyl radical, HCO_2. Two basic classes of parametrization are analyzed. In the first (vertical), the model Hamiltonian is constructed in such a way that it reproduces an ab initio surface near the geometry of the absorbing state in a spectroscopic transition; the second scheme (adiabatic) is designed to provide a faithful representation of the ab initio surface near the final state structures. The latter is better suited to treat energy level spacings, especially at relatively low energies, while the former may offer advantages in some cases where it may provide a more balanced description of the final states and/or features such as seams of conical intersections. For HCO_2, the most interesting and prominent feature of the vibronic coupling scheme is a strong coordinate dependence of the coupling between the two electronic states. This effect renders effectively useless parametrization approaches in which the linear coupling strength is assumed constant. Moreover, through selective softening of the $^2A_1$ state potential and corresponding reduction in its zero-point energy, this seemingly arcane property of the vibronic coupling in HCO_2 is principally responsible for the ground state of this molecule being $^2A_1$ instead of $^2B_2$, as the adiabatic potential energy surface minimum of the latter is some 500 cm^{-1} lower.

Keywords Formyloxyl · Vibronic · Quasidiabatic

Dedicated to Professor Pekka Pyykkö on the occasion of his 70th birthday and published as part of the Pyykkö Festschrift Issue.

K. Klein · J. Gauss
Institut für Physikalische Chemie,
Universität Mainz, 55099 Mainz, Germany
e-mail: gauss@uni-mainz.de

E. Garand
Department of Chemistry, Yale University,
New Haven, CT 06520, USA

T. Ichino · J. F. Stanton (✉)
Institute for Theoretical Chemistry,
Department of Chemistry and Biochemistry,
The University of Texas at Austin, Austin, TX 78712, USA
e-mail: jfstanton@mail.utexas.edu

D. M. Neumark
Department of Chemistry,
University of California, Berkeley, CA 94720, USA

1 Introduction

The formyloxyl radical (HCO_2) is the parent compound for organic carboxylate radicals, a class of transient molecules that are of interest in combustion and atmospheric processes [1]. The first detection of HCO_2 (as well as its isotopologue DCO_2) was reported by Kim et al. [2] by means of negative ion photoelectron spectroscopy of formate (HCO_2^-). Interpretation of the spectra was not straightforward, principally because the two lowest-lying σ states ($^2A_1$ and $^2B_2$, see Fig. 1) are nearly degenerate. Assignment of the photoelectron spectrum of HCO_2^- gave a splitting of 218 ± 121 cm^{-1} in favor of the $^2A_1$ state, but the DCO_2^- spectrum indicated that the ordering of electronic states is reversed in this isotopic species. Additional complications at higher energies in the spectra are due to presence of a third (π, $^2A_2$) state of the radical within a few hundred meV of the ground state level.

Knowledge of the state energies of formyloxyl has recently been advanced through use of the technique of slow electron velocity-map imaging (SEVI) [3]. This method uses varying laser energies to detach electrons from anions and

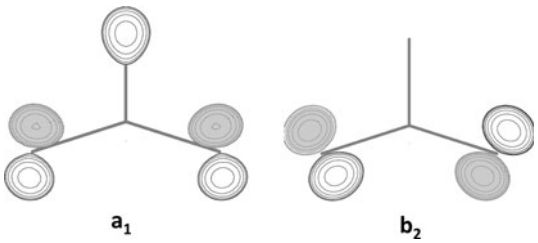

Fig. 1 The highest-lying occupied a_1 and b_2 orbitals of formate, detachment from which leads to the two electronic states featured in this study

analyze the velocity of those electrons which are in the near-threshold region. These data are assembled to generate negative ion photoelectron spectra with a significantly higher resolution than can be obtained with a conventional kinetic energy analyzer. SEVI spectra of HCO_2^- revealed that many of the broad bands assigned to individual vibronic levels in Ref. [2] are in fact composite features due to detachment to as many as four different neutral state levels. The great complexity of the HCO_2^- spectrum—due to the close-lying electronic states and the vibronic interaction between them—was such that its assignment was facilitated considerably by an analysis based on a model vibronic Hamiltonian [4].

The model used in the theoretical analysis of Ref. [4] was the venerable and powerful quasidiabatic framework of Köppel, Domcke, and Cederbaum (KDC) [5]. However, the complexity of the spectrum necessitated a rather sophisticated parametrization of the model Hamiltonian that extends well beyond the linear vibronic coupling (LVC) model that is most frequently used [6]. The LVC method is very simple to implement and provides a powerful means for obtaining *qualitative* insight into various kinds of electronic spectroscopy. It is, however, not sufficiently robust to predict level positions to better than about $100\,cm^{-1}$ and consequently unsuitable for assigning spectra like those of HCO_2^- and DCO_2^-. The parametrization used in Ref. [4] included quadratic as well as cubic and quartic terms in the (diabatic) potential expansion, all of which are needed to account for effects such as Duschinsky rotation and intrinsic anharmonicity[1]. In addition, the coupling strength between the states was treated with a bilinear model that allows the usual linear coupling constants to depend on the nuclear geometry to first order in totally symmetric displacements. Finally, the parametrization was done in such a way that the adiabatic surfaces obtained by diagonalization of the model are nearly coincident (through terms quadratic in displacement) with high-level ab initio surfaces in the vicinity of the final state minima[2]. This model of the two low-lying σ states of HCO_2 and DCO_2 gave an excellent agreement with the experimental spectra and allowed confident assignments to be made for every major feature within 2,000 cm^{-1} of the origins for both HCO_2 and DCO_2. Indeed, the agreement between the 22 level positions calculated from the model Hamiltonian and those measured in the SEVI experiments is typically in the range 10–20 cm^{-1}, which compares favorably to the accuracy usually achieved when high-level ab initio quantum chemistry is used to calculate infrared spectra [7, 8]. The SEVI work also resulted in more precise values for the electron affinity of HCO_2 ($3.4961 \pm 0.0010\,eV$) and the term energy for the $^2B_2$ state ($318 \pm 8\,cm^{-1}$). For the deuterated species, the improved experimental results and the theoretical analysis led to a reassignment of the origin, with the consequent finding that the $^2A_1$ state is lower in both isotopologues. The $^2B_2$ term energy in the deuterated species is $87 \pm 8\,cm^{-1}$ which, while significantly lower than that in the normal isotopic species, preserves the ordering of states found in HCO_2.

The purpose of this paper is twofold. First, a detailed description is given of how the vibronic Hamiltonian has been parametrized for formyloxyl. While the KDC model was first introduced more than a quarter century ago and has been described many times in the literature, the bulk of applications of this technique has tended toward qualitative interpretation of spectra (see e.g. Ref. [9–13]), rather than quantitative accuracy. To our knowledge, the parametrization used in Ref. [4] is among the most extensive yet used for the model, and a comprehensive discussion of the procedure is therefore warranted. Such a description is given in this paper and should enable others in the chemical physics community to easily adopt the approach to develop similar model Hamiltonians for other systems of spectroscopic interest. Second, performances of two different parametrization methods in the formyloxyl system are critically compared and assessed; the adiabatic parametrization, which is adopted in Ref. [4], and the vertical parametrization, which more directly obeys the diabatic potential expansion in the KDC model Hamiltonian. The

[1] Intrinsic anharmonicity is considered to be that which is associated with the quasidiabatic potential surfaces. This is to be distinguished from, for example, the pronounced anharmonicity associated with q_3, which is observed both experimentally and in the simulations of Ref. [4]. Given the rather modest magnitudes of the anharmonic force constants in Table 2 that involve q_3, this substantial anharmonicity is due largely to the vibronic coupling, which contributes to anharmonic force constants f_{3xx}, f_{33xx}, *etc*., where xx represents one of the coupling coordinate combinations 55, 56 and 66. For example, the values of 3_0^1 and 3_0^2 calculated for the $\tilde{X}^2A_2$ state with the VP4 model with and without the off-diagonal coupling terms are 572 and 1,069 cm^{-1} versus 621 and 1,240 cm^{-1}, respectively, revealing that essentially all of the anharmonicity in this coordinate arises from vibronic coupling effects.

[2] The parametrization used in Ref. [4] did not exactly reproduce the quadratic adiabatic force constants associated with the coupling coordinates q_5 and q_6, for reasons that are discussed just below Eq. (15).

discussion also concerns the extent to which simplification of the current parametrization—specifically to the LVC and so-called quadratic vibronic coupling (QVC) models—affects the predicted level positions and general appearance of spectra.

2 Theory

2.1 The quasidiabatic Hamiltonian

Vibronic coupling effects in the photoelectron spectrum of HCO_2^- are treated using the quasidiabatic representation popularized by Köppel et al. [5]. As a variety of detailed descriptions of the method already exist [5, 6], only a brief overview is given here. This is followed by details of the Hamiltonian parametrization, the latter being a principal focus of this work.

The treatment of vibronic interactions between strongly coupled electronic states in the adiabatic representation is complicated by the extraordinary sensitivity of the associated electronic wave functions to nuclear coordinates in such regions [5]. In principle, this problem can be avoided via transformation to a diabatic representation, where the nuclear kinetic energy is diagonal in the electronic basis and the potential energy part of the Hamiltonian takes a non-diagonal form. This is, however, an idealization since strictly diabatic representations exist only in an extreme limit and practical calculations can only approximate this situation. Nevertheless, a pedagogically useful and truly diabatic (strictly diagonal) nuclear kinetic energy operator can be achieved if the wave function of the molecule is represented by a product of electronic wave functions $\psi_I(\mathbf{r};\mathbf{R}_0)$ with electronic coordinates $\mathbf{r}$ at a "frozen" reference geometry $\mathbf{R}_0$ and vibrational wave functions $\chi_{v,I}(\mathbf{R})$ depending on nuclear coordinates $\mathbf{R}$ (see also ref. [6])

$$\Psi(\mathbf{r},\mathbf{R}) = \sum_I \psi_I(\mathbf{r};\mathbf{R}_0) \sum_v \chi_{v,I}(\mathbf{R}). \tag{1}$$

In this (static Born–Huang) basis, the blocks of the molecular Hamiltonian assume the following structure

$$\mathbf{H} = \begin{pmatrix} E_0\mathbf{1} & 0 & \cdots \\ 0 & E_A\mathbf{1} & \cdots \\ \vdots & \vdots & \ddots \end{pmatrix} + \begin{pmatrix} \mathbf{T}_n & 0 & \cdots \\ 0 & \mathbf{T}_n & \cdots \\ \vdots & \vdots & \ddots \end{pmatrix} + \begin{pmatrix} \mathbf{V}_{00} & \mathbf{V}_{0A} & \cdots \\ \mathbf{V}_{A0} & \mathbf{V}_{AA} & \cdots \\ \vdots & \vdots & \ddots \end{pmatrix}. \tag{2}$$

The electronic ground state is denoted by 0 and excited states by A, B, etc. E_I are the eigenvalues of the electronic Hamiltonian obtained at the reference geometry $\mathbf{R}_0$, $\mathbf{1}$ is a unit matrix having the dimension of the vibrational basis χ_v, and $\mathbf{T}_n$ is the matrix of the nuclear kinetic energy in the vibrational basis. The contributions to the effective potential energy matrices $\mathbf{V}_{IJ}$ are given by the matrix elements $\langle\psi_I(\mathbf{r};\mathbf{R}_0)\chi_{v,I}(\mathbf{R}) \mid \hat{H}_{\mathrm{el}} \mid \psi_J(\mathbf{r};\mathbf{R}_0)\chi_{v',J}(\mathbf{R})\rangle$.

Typically, only a very few electronic states account for the principal failure of the adiabatic model when it does not properly describe a spectrum. Conceptually, these troublesome states may be isolated from the rest of the electronic states in the idealized diabatic picture above by block diagonalization of the potential [5]. This procedure allows the frozen diabatic electronic wavefunctions of the model above to relax with nuclear coordinate displacements; in particular, this—again conceptually—builds in the usual "following of the nuclei" behavior and most of the simple variation of wave functions anticipated from qualitative molecular orbital theory. However, this mixing of the frozen electronic states spoils the rigorously diagonal nature of the nuclear kinetic energy operator above, and the resulting electronic basis is termed "quasidiabatic" [14]. If the states that are isolated from the rest are well-chosen, however, the residual off-diagonal kinetic energy coupling is small. In other words, when calculating *vibronic* energy levels of such a system, one can ignore the residual off-diagonal coupling terms in the kinetic energy operator with the same confidence associated with ignoring non-Born-Oppenheimer effects for calculation of *vibrational* energy levels in "simple" electronic states (like those found in most closed-shell molecules). In most applications of the KDC model, as well as our work on formyloxyl and other species, the nuclear coordinates are taken to be a set of normal coordinates in the dimensionless representation, using a common origin and set of coordinates for all electronic states under consideration. While more elaborate coordinate choices have been advocated [15, 16], the rather simple choice of a common set of normal coordinates is nevertheless adequate for treating formyloxyl—which is a relatively difficult vibronic coupling problem—with quantitative accuracy. Moreover, the discussion of the parametrization below is rendered simpler by this coordinate choice.

2.2 Parametrization

Before projection onto the vibrational basis, blocks of the potential energy matrix in the quasidiabatic representation are expanded in polynominals about a well-defined reference state; the adiabatic potential energy surfaces can then be obtained via point-by-point diagonalization. In the present study, the origin of the coordinate system corresponds to the formate geometry and the nuclear coordinates are the (dimensionless) normal coordinates of the anion. This choice is made because the Hamiltonian is being used

to study the photoelectron spectrum of formate; use of the coordinates of the state that absorbs the radiation greatly facilitates the calculation of the spectral intensities when the Lanczos procedure is used to obtain selected eigenvalues of the Hamiltonian [17]. For formyloxyl, this choice of coordinates has the additional advantage that the geometry of the anion is intermediate (in terms of both bond angles and bond lengths, see top of Table 1) between those of the final states of interest. This choice of origin also tends to ameliorate problems associated with the use of (necessarily truncated) polynomial expansions in the coordinates, since the "important" parts of nuclear configuration space are, in some sense, close to the origin.

For any two-state system like that which most appropriately describes the low-lying vibronic states of HCO_2, the potential matrix can be written in the general form

$$\mathbf{V} = \begin{pmatrix} \Delta_0^A + \sum_i F_i^A q_i + \frac{1}{2}\sum_{ij} F_{ij}^A q_i q_j + \cdots & \sum_i \lambda_i^{AB} q_i + \cdots \\ \sum_i \lambda_i^{BA} q_i + \cdots & \Delta_0^B + \sum_i F_i^B q_i + \frac{1}{2}\sum_{ij} F_{ij}^B q_i q_j + \cdots \end{pmatrix}, \tag{3}$$

which holds so long as the states A and B have different symmetries. The diagonal blocks of $\mathbf{V}$—which represent the corresponding *quasidiabatic potential energy surfaces*—contain force constants F associated with the normal modes $i, j, \ldots$. Note that there is a linear term, which is due to the fact that the origin of the coordinate system is not necessarily (and is certainly not here) coincident with local minima on the corresponding quasidiabatic surfaces. The Δ_0 parameters are the vertical electron detachment energies of formate to states A and B at the reference (anion) geometry. The off-diagonal block of $\mathbf{V}$ describes the coupling between the quasidiabatic electronic states and represents the most challenging and arguably the most important part of the parametrization. Diagonalization of $\mathbf{V}$ gives the adiabatic surfaces v_a and v_b which are coincident with the corresponding quasidiabatic potentials at the reference geometry R_0 as well as all structures displaced from it along (exclusively) totally symmetric coordinates. Along the coupling coordinates, the correspondence is lost, and the mapping between quasidiabatic and adiabatic states is completely scrambled in the vicinity of conical intersections.

For HCO_2, the two lowest electronic states have different symmetries, and the conceptual block diagonalization of the diabatic Hamiltonian mentioned in the previous section is such that the corresponding quasidiabatic and adiabatic states are coincident in the totally symmetric

Table 1 Fidelity of adiabatic potential energy surfaces associated with the various parametrization schemes

	$^2A_1$						$^2B_2$					
	LVC	VP2	VP4	AP2	AP4	Ab init	LVC	VP2	VP4	AP2	AP4	Ab init
q_1	−0.062	−0.011	0.027	a	a	0.075	−0.365	−0.314	−0.246	a	a	−0.245
q_2	−0.768	−1.394	−1.596	a	a	−1.594	0.793	0.631	0.413	a	a	0.437
q_3	−1.347	−1.813	−2.004	a	a	−1.998	2.313	4.061	3.567	a	a	3.524
ν_1	2,631	2,644	2,378	a	a	2,333	2,631	2,715	3,104	a	a	3,106
ν_2	1,349	1,186	1,178	a	a	1,176	1,349	1,398	1,496	a	a	1,474
ν_3	758	704	650	a	a	655	758	568	626	a	a	644
ν_5	1,445	1,400	1,410	a	a	1,656	1,446	1,514	1,499	a	a	1,292
ν_6	125i	852i	760i	a	a	153i	372	1,052	933	a	a	1,093
E_{stab}	−1,090	−1,648	−1,769	−1,642	−1,775	−1,768	−2,626	−4,047	−3,646	−4,094	−3,628	−3,634
E_{rel}	199	1,062	540	1,115	516	539	0	0	0	0	0	0
Δ_e	6,774	9,830	10,904	13,105	10,566	10,945	7,039	13,004	10,792	10,748	10,709	10,866

	Minimum on seam of conical intersections					
	LVC	VP2	VP4	AP2	AP4	Ab initio
$q^{xs}{}_1$	−0.208	−0.198	−0.184	−0.261	−0.179	−0.184
$q^{xs}{}_2$	−0.010	−0.026	−0.027	0.058	−0.040	−0.026
$q^{xs}{}_3$	0.430	0.436	0.440	0.347	0.452	0.440
E^{xs}	522	506	509	398	512	510

Given above are the displacements from the reference (anion) structure, harmonic frequencies, stabilization energies (E_{stab}) (the separation between the anion geometry and the equilibrium geometries), the relative adiabatic energies (E_{rel}), and the vertical gaps at the equilibrium geometries (Δ_e). All values are in cm^{-1}; displacements are in terms of the reduced normal coordinates of the anion. The vertical separation used here is given by the unadjusted ab initio value of 1337 cm^{-1} with the $^2B_2$ energy higher. Also given are the geometries of the minimum on the (C_{2v}) seam of conical intersections, and its energy relative to the $^2A_1$ state at the anion geometry

[a] Agrees with the ab initio result, by construction

subspace of possible nuclear geometries, as just mentioned. In other words, all constants in the corresponding diagonal blocks of **V** (see Eq. 3) associated *only* with totally symmetric coordinates are equal to those obtained in the adiabatic representation, *viz.*

$$F_i^A = \left(\frac{\partial v_a}{\partial q_i}\right)_{R_0}; \quad F_{ij}^A = \left(\frac{\partial^2 v_a}{\partial q_i \partial q_j}\right)_{R_0}; \quad \cdots \qquad \forall\, i,j\cdots \in \Gamma_{\text{tot.symm.}}, \tag{4}$$

with analogous expressions for state B. It is thus appropriate to generate these parameters using standard ab initio quantum-chemical calculations. Simple considerations of symmetry also dictate that, for asymmetric tops, nonzero linear constants F_i occur only when q_i is a totally symmetric mode. Quadratic and higher-order constants vanish unless the direct product of the irreducible representations associated with the modes in the subscripts is the totally symmetric representation. For example, nonzero quadratic constants F_{ij} require that q_i and q_j belong to the same symmetry species. In passing, we note that these restrictions *do not* apply for degenerate states of spherical and symmetric tops, where the Jahn–Teller interaction leads to nonzero linear terms in the diagonal quasidiabatic potential. These are associated with selected non-symmetric coordinates; in this case, the quadratic and higher-order terms are considerably more complicated, as well [18–20].

For the interacting states in HCO_2, the quadratic constants fall into two classes. In the first, both indices correspond to totally symmetric modes and the corresponding constants are precisely equal to the adiabatic values obtained in quantum-chemical calculations, for the reason discussed above. The second type of constant involves indices that belong to the same, but non-totally symmetric, irreducible representation. If the individual symmetries of these indices are different from the coupling modes active in the model Hamiltonian, they are again the same as the adiabatic values. However, when they correspond to the symmetry of the coupling modes (given by direct products of the symmetries of the electronic states under consideration, i.e., $a_1 \times b_2 = b_2$), the diabatic force constants F_{ij} and the adiabatic force constants do not coincide because of the off-diagonal potential energy coupling. It is straightforward to show that the diabatic constants of this type are given—exactly within the imposed structure of the Hamiltonian—by

$$F_{ij}^{A(B)} = \left(\frac{\partial^2 v_{a(b)}}{\partial q_i \partial q_j}\right)_{R_0} + \frac{2\lambda_i\lambda_j}{\Delta_{A(B)}^{B(A)}}, \quad \Delta_A^B = E_B - E_A \tag{5}$$

$$= f_{ij}^{A(B)} + \frac{2\lambda_i\lambda_j}{\Delta_{A(B)}^{B(A)}}, \tag{6}$$

where upper- and lower-case force constants designate quasidiabatic and adiabatic values, respectively. Here, the vertical energy difference Δ_A^B is equal to that between the coupled states A and B at the reference geometry.

The λ parameters that appear in the off-diagonal blocks of the potential describe the vibronic coupling between the different radical states of HCO_2. These are formally given as derivatives of matrix elements of the electronic Hamiltonian between the quasidiabatic electronic states $\psi^{A,B,\ldots}$

$$\lambda_i^{AB} = \frac{\partial}{\partial q_i}\langle\psi^A|\hat{H}|\psi^B\rangle, \quad \lambda_{ij}^{AB} = \frac{\partial^2}{\partial q_i \partial q_j}\langle\psi^A|\hat{H}|\psi^B\rangle, \quad \cdots. \tag{7}$$

The resulting linear coupling constants λ_i are, again from symmetry considerations, only nonzero if the irreducible representation of the mode q_i is given by the direct product of any pair of coupled target states A and B. Quadratic terms λ_{ij} vanish unless the product of the symmetries associated with modes q_i and q_j is equal to $\Gamma_A \times \Gamma_B$. A particularly important subset of the quadratic coupling constants are those in which one index corresponds to a coupling coordinate and the other to a totally symmetric coordinate. These bilinear terms, which were included in the parametrization for HCO_2 in Ref. [4], allow the effective linear coupling strength to vary with geometry, an effect that turns out to be of vital importance in HCO_2 [21].[3]

The above provides a brief overview of the structure of the vibronic Hamiltonian and an interpretation of the meaning and definitions of each term. In the next section, the specific procedure used to determine the various parameters for the HCO_2 molecule is discussed.

3 Computational details

3.1 Model potential for HCO_2: diagonal blocks

The HCO_2 system is treated in C_{2v} symmetry, where there are six non-degenerate normal modes. Three of these have a_1 symmetry (the CH stretch ν_1, the symmetric CO stretch ν_2 and the OCO bend ν_3), one has b_1 symmetry (the out-of-plane "umbrella" mode ν_4), and two have b_2 symmetry (the out-of-phase CO stretch ν_5 and the HCO wagging motion ν_6). The b_2 modes couple the low-lying $^2A_1$ and $^2B_2$ states, while the umbrella mode couples the $^2A_2$ and the $^2B_2$ states. The latter coupling was not explicitly included in any of the calculations in this paper (apart from its contribution to the zero-point energy) since this research focuses only on the two lowest-lying states of HCO_2. The model potential is then given by

[3] Significant effects of bilinear couplings on the potential energy surfaces have been found in other systems as well. See, for example, Ref. [21].

$$\mathbf{V} = \begin{pmatrix} A & X \\ X & B \end{pmatrix}, \tag{8}$$

with the diagonal blocks

$$A = \Delta_0^{A_1} + \sum_i F_i^{A_1} q_i + \frac{1}{2}\sum_{ij} F_{ij}^{A_1} q_i q_j + \frac{1}{6}\sum_{ijk} F_{ijk}^{A_1} q_i q_j q_k + \frac{1}{24}\sum_{ijkl} F_{ijkl}^{A_1} q_i q_j q_k q_l \tag{9}$$

$$B = \Delta_0^{B_2} + \sum_i F_i^{B_2} q_i + \frac{1}{2}\sum_{ij} F_{ij}^{B_2} q_i q_j + \frac{1}{6}\sum_{ijk} F_{ijk}^{B_2} q_i q_j q_k + \frac{1}{24}\sum_{ijkl} F_{ijkl}^{B_2} q_i q_j q_k q_l \tag{10}$$

and a term that accounts for the coupling between the different electronic states:

$$X = \sum_i \lambda_i^{A_1 B_2} q_i + \frac{1}{2}\sum_{ij} \lambda_{ij}^{A_1 B_2} q_i q_j. \tag{11}$$

As a further simplification, the diabatic potential is limited to quadratic terms, except for the F_{ijk} and F_{ijkl} constants, where only those constants are retained for which all indices belong to the totally symmetric representation (q_1, q_2 and q_3).

The parameters above can be obtained in at least two different ways. In the so-called vertical parametrization [22], they are chosen to be equivalent to the derivatives with respect to the normal coordinates, calculated at the reference geometry (see Eq. (4)). In such an approach, diagonalization of $\mathbf{V}$ will precisely reproduce the adiabatic potential energy surfaces in the immediate vicinity of the reference geometry. This condition—where the adiabatic potentials are the "correct" ones only near the vertical geometry—can be problematic when one wants to accurately calculate final state energy levels since it does not necessarily follow that the adiabatic potentials from the model Hamiltonian will accurately reproduce the ab initio potentials near the minimum of the target states. Nevertheless, this choice is adequate for processes in which geometrical changes between the reference and final states are rather small, but presumably not for cases like HCO_2, where they are considerably larger.[4]

[4] In terms of internal coordinates, the geometries of the anion and the diabatic minima for the $^2A_1$ and $^2B_2$ states of HCO_2 are (in Angstroms and degrees): $r_{CO} = 1.255$, $r_{CH} = 1.133$, $\theta_{OCO} = 130.6$ (anion); $r_{CO} = 1.228$, $r_{CH} = 1.160$, $\theta_{OCO} = 144.8$ ($^2A_1$); $r_{CO} = 1.257, r_{CH} = 1.093$, $\theta_{OCO} = 112.5$ ($^2B_2$). Note that the qualitative difference in geometry between the two neutral states is the same as that found in the related NO_2 radical. In addition, the minimum on the seam of conical intersections occurs at: $r_{CO} = 1.251$, $r_{CH} = 1.111$, $\theta_{OCO} = 128.4$.

In an alternative approach, known as the "adiabatic parametrization" [22], force fields are calculated at the minima of the final states and transformed into the basis of reduced normal coordinates of the reference state. Provided that the displacements of the target states relative to the reference state are such that the point group symmetry of the latter is preserved, the diabatic force constants associated with the "adiabatic" parametrization are related to those calculated at the minimum energy geometries $\tilde{F}$ by the straightforward linear transformations

$$F_i^A = -\sum_j \tilde{F}_{ij}^A q_j^A + \frac{1}{2}\sum_{jk} \tilde{F}_{ijk}^A q_j^A q_k^A - \frac{1}{6}\sum_{jkl} \tilde{F}_{ijkl}^A q_j^A q_k^A q_l^A \tag{12}$$

$$F_{ij}^A = \tilde{F}_{ij}^A - \sum_k \tilde{F}_{ijk}^A q_k^A + \frac{1}{2}\sum_{kl} \tilde{F}_{ijkl}^A q_k^A q_l^A \tag{13}$$

$$F_{ijk}^A = \tilde{F}_{ijk}^A - \sum_l \tilde{F}_{ijkl}^A q_l^A \tag{14}$$

$$F_{ijkl}^A = \tilde{F}_{ijkl}^A, \tag{15}$$

where the coordinate vector $\mathbf{q}^\mathbf{A}$ is the displacement from the reference geometry R_0 to the minimum on the diabatic potential surface of state A. Note that the linear terms $\tilde{F}_i^A$ vanish here.

Here, we elaborate slightly on the procedure used to parametrize the quadratic force constants associated with modes involved in the vibronic coupling, specifically ν_5 and ν_6 in the case of the coupling between the $\tilde{X}^2A_1$ and $\tilde{A}^2B_2$ states of HCO_2. In Ref. [4], these constants were taken from Eq. (5), using the adiabatic force constants and vertical energy differences obtained in high level ab initio calculations. This method is consistent with the ab initio spirit of the approach, but there is a way to "improve" this procedure, at least insofar as the fidelity with which the ab initio potential energy surfaces are reproduced by the model. The problem that can occur is that the earlier procedure will give the ab initio value of the adiabatic force constants f_{55}, f_{56}, and f_{66} only if the vertical energy separation at the geometries of the $^2A_1$ and $^2B_2$ states given by the model Hamiltonian is the same as that from the ab initio calculations. What can be done instead is to use the energy difference from the model Hamiltonian (which depends only on the totally symmetric force fields of the two states) in Eq. (5). This alternative procedure precisely reproduces the ab initio force field for the coupling modes; together with the method outlined in the previous paragraph, it guarantees that the harmonic force field of the final states obtained from the adiabatic surfaces corresponding to the model Hamiltonian will be identical to that from the ab initio calculations. While differences between the two approaches are expected to be small when the

expansions of Eq. (9) are extended through quartic terms, they can become significant when the terms associated with the totally symmetric coordinates are truncated more severely. As a major aim of the present paper is to compare various methods for parametrization, we will choose this latter approach for fixing the quasidiabatic force constants for the coupling modes; otherwise, the perceived importance of using quartic, rather than quadratic, expansions of the potential would be exaggerated.

For the determination of the adiabatic potential surfaces, coupled-cluster singles and doubles calculations with a perturbative treatment of triples (CCSD(T)) [23] were used. The reference function for the calculations was an unrestricted Hartree–Fock (UHF) determinant, using the atomic natural orbital (ANO) basis set of Taylor and Almlöf [24]. The basis was truncated to 4*s*3*p*2*d*1*f* on C and O, and 4*s*2*p*1*d* on H (approximately of valence triple-zeta size), which will hereafter be referred to as ANO1. All electronic structure calculations using the ANO1 basis set did not include core electrons in the correlation treatment. The geometries were determined using an UHF-CCSD(T)/ANO1 optimization procedure based on analytic gradients [25]. The quadratic force constants were obtained from harmonic frequency calculations based on analytic second derivatives [26], while the cubic and quartic parameters were determined from least-square fits of a $9 \times 9 \times 9$ energy grid (729 points) at displacements up to $q = 0.4$ along the (totally symmetric) reduced normal coordinates of the anion, centered about the minimum energy geometry of the neutral states (adiabatic parametrization) or the anion (vertical parametrization).

In order to analyze the sensitivity of the level positions and the general appearance of the spectrum to the parametrization, a number of choices for the quasidiabatic potential matrix were used. In the first, the linear, quadratic, cubic, and quartic terms on the diagonal blocks associated only with totally symmetric nuclear displacements were taken to be those calculated at the *vertical* (anion) geometry; this parametrization is designated as VP4 (vertical parametrization with up to quartic constants) to distinguish it from that in which the force constants reproduce the adiabatic surfaces at the minima (that generated via Eq. (12)), which is called AP4 (adiabatic parametrization). All parameters used in the Hamiltonians of this work are collected in Tables 2, 3 and 4. Of course, in the limit that the

Table 2 Force constants (in cm^{-1}) for the HCO_2 molecule

	Adiabatic		Vertical			Adiabatic		Vertical	
	$^2A_1$	$^2B_2$	$^2A_1$	$^2B_2$		$^2A_1$	$^2B_2$	$^2A_1$	$^2B_2$
Δ_0^a	0	1429	0	1,429	F_{133}	28	−11	62	2
F_1	0	0	162	959	F_{123}	−20	−31	−33	−35
F_2	0	0	1,036	−1,070	F_{223}	140	47	113	109
F_3	0	0	1,021	−1,753	F_{233}	−63	20	−24	18
F_{11}	2,048	3,651	2,656	2,799	F_{1111}	1,062	1,528	1,196	1,231
F_{22}	959	1,631	1,007	1,455	F_{2222}	−3	45	12	8
F_{33}	755	565	719	427	F_{3333}	−8	15	7	4
F_{12}	250	−292	43	−109	F_{1112}	−80	−113	−72	−99
F_{13}	55	−53	40	−3	F_{1113}	−23	−35	−22	−29
F_{23}	−330	158	−203	29	F_{1122}	3	0	−5	5
F_{55}	1,915	1,533	1,242	1,434	F_{1133}	5	0	4	0
F_{66}	920	1,234	858	1,647	F_{1123}	3	0	0	0
F_{56}	−308	239	−323	252	F_{1222}	8	5	10	12
F_{111}	−1,894	−2,519	−2,140	−2,027	F_{1223}	−1	9	4	7
F_{222}	−107	−338	−162	−218	F_{1233}	−9	2	−5	−3
F_{333}	9	57	26	19	F_{1333}	−4	2	−5	−4
F_{112}	211	192	220	165	F_{2223}	−28	−31	−31	−38
F_{113}	48	67	62	58	F_{2233}	19	−19	3	−4
F_{122}	−92	−21	−75	−54	F_{2333}	10	−6	8	8

The vertical force constants have been evaluated at the equilibrium geometry of the HCO_2^- anion, the adiabatic parameters at the equilibrium geometry of the corresponding neutral states, both using the UHF-CCSD(T)/ANO1 method. In the vertical case, the parameters above are those that go into the Hamiltonian; for the adiabatic parametrization, the Hamiltonian parameters are generated from these and the displacements listed in Table 1 using Eqs. (12)–(15) (the constants above represent the $\tilde{F}$ parameters in those equations). The vertical energy gap includes the effect of zero-point energy in the ν_4 mode

[a] Includes a correction for the zero-point energy of q_4

potential is truly quartic, the two parametrizations are identical; differences between the two sets of parameters (see Table 4) are indicative of the departure from this idealized situation.

A simplified potential in which the harmonic approximation is applied to the adiabatic potential surface, as in Ref. [22], is also used and denoted as AP2 in the context of this work

$$F_i^A = -\sum_j \tilde{F}_{ij}^A q_j^A \tag{16}$$

$$F_{ij}^A = \tilde{F}_{ij}^A. \tag{17}$$

Table 3 The (quasi)diabatic coupling constants λ for the ν_5 and ν_6 coupling modes of HCO_2

	$\lambda_{\text{vertical}}$	$\lambda_{\text{adiabatic}}$
λ_5^0	2,198	2,115
λ_{15}	−34	−13
λ_{25}	2	1
λ_{35}	5	2
λ_6^0	840	894
λ_{16}	15	16
λ_{26}	−156	−163
λ_{36}	−89	−93

The force constants corresponding to Eq. (24) and Eqs. (27) and (28) (linear model) are given in cm^{-1}

Similarly to VP4, a VP2 parametrization is achieved when the vertical harmonic potential, including F_i and F_{ij}, is determined at the reference geometry. Finally, in the LVC parametrization, only the linear terms F_i from VP2 are included in the diagonal blocks; the quadratic force constants are taken to be those of the anion.

The coupling constants associated with these parametrizations are as follows: in all treatments other than LVC, linear and bilinear constants are included. These are chosen in AP2 and AP4 so that the linear coupling constants (calculated as described below) are reproduced exactly at the minimum energy geometries of the final states; in VP2 and VP4, they are the linear and bilinear coupling constants determined at the anion geometry. Coupling constants in the LVC model are limited to the linear terms λ_5 and λ_6 evaluated at the anion geometry.

3.2 Model potential for HCO_2: off-diagonal block

The coupling constants between the vibronically mixed final states were determined using the analytic procedure introduced in Ref. [27]. In this work, the electronic wave functions of the neutral states are based on the so-called equation-of-motion coupled-cluster method for ionization potentials (EOMIP-CC) [28, 29], using the singles and doubles approximation (EOMIP-CCSD). The electronic wavefunction in this method is obtained by diagonalization of the similarity-transformed Hamiltonian

Table 4 Diabatic force constants (in cm^{-1}) involving totally symmetric coordinates only for the HCO_2 molecule

	Adiabatic		Vertical			Adiabatic		Vertical	
	$^2A_1$	$^2B_2$	$^2A_1$	$^2B_2$		$^2A_1$	$^2B_2$	$^2A_1$	$^2B_2$
F_1	158	921	162	959	F_{223}	133	130	113	109
F_2	1,051	−1,031	1,036	−1,070	F_{233}	−12	50	−24	18
F_3	1,025	−1,752	1,021	−1,753	F_{1111}	1,062	1,528	1,196	1,231
F_{11}	2,662	2,803	2,656	2,799	F_{2222}	−3	45	12	8
F_{22}	1,019	1,438	1,007	1,455	F_{3333}	−8	15	7	4
F_{33}	712	433	719	427	F_{1112}	−80	−113	−72	−99
F_{12}	35	−103	43	−109	F_{1113}	−23	−35	−22	−29
F_{13}	36	31	40	−3	F_{1122}	3	0	−5	5
F_{23}	−185	−13	−203	29	F_{1133}	5	0	4	0
F_{111}	−2,147	−1,973	−2,140	−2,027	F_{1123}	3	0	0	0
F_{222}	−168	−247	−162	−218	F_{1222}	8	5	10	12
F_{333}	9	7	26	19	F_{1223}	−1	9	4	7
F_{112}	228	164	220	165	F_{1233}	−9	2	−5	−3
F_{113}	65	58	62	58	F_{1333}	−4	2	−5	−4
F_{122}	−81	−55	−75	−54	F_{2223}	−28	−31	−31	−38
F_{133}	5	−19	62	2	F_{2233}	19	−19	3	−4
F_{123}	−40	−42	−33	−35	F_{2333}	10	−6	8	8

The close correspondence of those obtained in both adiabatic and vertical parametrizations shows that a quartic representation of the potential is a reasonably good one over the relevant range of coordinates

$$\bar{H} \equiv \exp(-T) H \exp(T), \tag{18}$$

where T is the operator that maps the reference state (anion, in this case) Hartree–Fock determinant into the correlated wavefunction. In EOMIP-CCSD, this operator T is obtained by solving the usual coupled-cluster singles and doubles (CCSD) equations [30], and the final state wavefunctions are given by[5]

$$|\,\psi_{\mathrm{EOM}}\rangle = \hat{R} e^{\hat{T}}\,|\,\psi_{\mathrm{HF}}\rangle, \tag{19}$$

where the ionization operator $\hat{R}$ (the right-hand eigenvector of $\bar{H}$) is defined by

$$\hat{R} = \sum_i r_i \hat{a}_i + \frac{1}{2}\sum_{ija} r_{ij}^{a} \hat{a}_i \hat{a}_a^{\dagger} \hat{a}_j + \cdots \tag{20}$$

with amplitudes $r_{ij\ldots}^{a\ldots}$ and second quantization operators $\hat{a}_p$ and $\hat{a}_p^{\dagger}$.

With the analogously defined left-hand wave function $\langle\psi_{\mathrm{EOM}}\,| = \langle\psi_{\mathrm{HF}}\,|\,\hat{L}e^{-\hat{T}}$ the general definition of the coupling constant is given as the derivative of the Hamiltonian matrix element with respect to the reference normal coordinates

$$\lambda_i^{AB} = \left(\frac{\partial}{\partial q_i}\langle\psi_{\mathrm{HF}}|\hat{L}_A e^{-\hat{T}}\hat{H}e^{\hat{T}}\hat{R}_B|\psi_{\mathrm{HF}}\rangle\right)_{\hat{L}_A,\hat{R}_B}, \tag{21}$$

i.e., with constant $\hat{L}_A$ and $\hat{R}_B$. Applying general EOMIP gradient theory [29], the expression can be cast into

$$\begin{aligned}\lambda_i^{AB} = &\left\langle \psi_{\mathrm{HF}}\middle|\hat{L}_A e^{-\hat{T}}\frac{\partial\hat{H}}{\partial q_i}e^{\hat{T}}\hat{R}_B\middle|\psi_{\mathrm{HF}}\right\rangle \\ &+\left[(E_A - E_B)\langle\psi_{\mathrm{HF}}|\hat{L}_A\hat{R}_B|P\rangle\right. \\ &\left.+\left\langle\psi_{\mathrm{HF}}\middle|\hat{L}_A e^{-\hat{T}}\hat{H}e^{\hat{T}}\middle|Q\right\rangle\langle Q|\hat{R}_B|P\rangle\right]\left\langle P\middle|\frac{\partial\hat{T}}{\partial q_i}\middle|\psi_{\mathrm{HF}}\right\rangle\end{aligned} \tag{22}$$

with the projection space P including singly and doubly excited determinants in the case of CCSD. The equation above can be simplified using the Dalgarno-Stewart interchange theorem [31]; the analytic linear coupling constants are then given by

$$\begin{aligned}\lambda_i^{AB} = &\left\langle \psi_{\mathrm{HF}}\middle|\hat{L}_A e^{-\hat{T}}\frac{\partial\hat{H}}{\partial q_i}e^{\hat{T}}\hat{R}_B\middle|\psi_{\mathrm{HF}}\right\rangle \\ &+\left\langle\psi_{\mathrm{HF}}\middle|\hat{Z}e^{-\hat{T}}\frac{\partial\hat{H}}{\partial q_i}e^{\hat{T}}\middle|\psi_{\mathrm{HF}}\right\rangle.\end{aligned} \tag{23}$$

The EOMIP wave functions used in this ansatz are "quasidiabatic" due to the fact that $\hat{R}$ and $\hat{L}$ are not allowed to relax along the coupling coordinates q_i. For the model potential of HCO_2, the λ_i were determined as described above, using the EOMIP-CCSD method and the double-zeta plus polarization (DZP) basis set [32], with all electrons correlated.[6] The choice of the DZP basis set is motivated mostly because it deals better with core correlation effects than the atomic natural orbital basis sets. This is important in the present work because the implementation of analytic coupling constant calculations is currently restricted to all electron calculations. The bilinear coupling constants (λ_{ij}, with one index corresponding to totally symmetric nuclear coordinates) are calculated by numerical differentiation of the analytic λ_i with respect to the totally symmetric normal coordinates.

As stated above, in the vertical picture, the linear and bilinear coupling constants are simply those evaluated, as above, at the geometry of the anion. In the adiabatic pictures AP2 and AP4, the procedure is more involved, since achievement of the goal—to have the coupling terms in the potential coincide with the ab initio values at the minimum energy C_{2v} geometries of the final states using a bilinear parametrization of the constants—does not have a unique solution. The coordinate-dependent linear coupling constant for a given mode, q_i, is given in this approximation by

$$\lambda_i(\mathbf{q}) = \lambda_i^0 + \sum_{\substack{j,\\ \text{tot.sym.}}} \lambda_{ij} q_j. \tag{24}$$

Therefore, for the two states A and B and the three totally symmetric coordinates q_1, q_2, and q_3, the following two equations must be satisfied

$$\lambda_i(\mathbf{q}^A) = \lambda_i^0 + \lambda_{i1}q_1^A + \lambda_{i2}q_2^A + \lambda_{i3}q_3^A \tag{25}$$

$$\lambda_i(\mathbf{q}^B) = \lambda_i^0 + \lambda_{i1}q_1^B + \lambda_{i2}q_2^B + \lambda_{i3}q_3^B. \tag{26}$$

In the above, λ_i^0 represents the coupling constant at the vertical geometry (treated as an unknown here), and the coordinate vectors $\mathbf{q}^A$ and $\mathbf{q}^B$ are the minimum energy geometries of the diabatic potentials for states A and B. The coordinate vectors and the coupling constants at the diabatic minima are taken from the ab initio calculations, and the other parameters are used in the fitting procedure. Unfortunately, the number of unknowns here exceeds the number of equations; a procedure that leads to a unique solution is to make the assumption

$$\lambda_i(\mathbf{q}^A) = \lambda_i^0 + \alpha\left(\lambda_{i1}^0 q_1^A + \lambda_{i2}^0 q_2^A + \lambda_{i3}^0 q_3^A\right) \tag{27}$$

$$\lambda_i(\mathbf{q}^B) = \lambda_i^0 + \alpha\left(\lambda_{i1}^0 q_1^B + \lambda_{i2}^0 q_2^B + \lambda_{i3}^0 q_3^B\right), \tag{28}$$

where the bilinear terms λ_{ij}^0 are those calculated at the anion geometry (those used in the vertical parametrization) and α can be regarded as an empirical scaling parameter. This

[5] Due to the intrinsically non-Hermitian nature of coupled-cluster theory, coupling constants λ_i^{AB} and λ_i^{BA} are not equal. In this work, the coupling constants that were used were the geometric mean of the two, both of which agreed to within 1% in all cases.

[6] An alternative parametrization method has been reported that utilizes MCSCF wavefunctions to analytically evaluate derivative couplings; see, for example, Ref. [15].

second set of equations can easily be solved for the unknown parameters α and λ_i^0; the latter, together with the scaled (by α) vertical bilinear constants, are used in the Hamiltonian.

This concludes the discussion of the various parametrizations of the KDC Hamiltonian used in this work. All electronic structure calculations presented in this paper were performed using the CFOUR program system[7]; calculations of the spectra and features of the model potential energy surfaces used the XSIM module, which is part of a development version of CFOUR.

4 Results and discussion

In the following, a brief analysis is given of the various parametrization schemes used for the two-state ($^2A_1$ and $^2B_2$) vibronic Hamiltonian for HCO_2. First, the adiabatic potential energy surfaces given by the Hamiltonians are analyzed; this is followed by a presentation and discussion of corresponding negative ion photoelectron spectral simulations.

4.1 Adiabatic potential energy surfaces

Parameters that characterize the adiabatic potential energy surfaces v_a and v_b associated with the $\tilde{X}^2A_1$ and $\tilde{A}^2B_2$ states of HCO_2 are listed in Table 1. Collected there are the harmonic frequencies, geometries (in terms of the reduced normal coordinates of the anion) (see footnote 4), and various energy differences as well as the geometries and energies of the minimum on the seam of conical intersections between the two states.

All of the models used here—LVC, VP2, VP4, AP2, and AP4—give the same qualitative picture of the potential energy surfaces for the two states. Specifically, while they are only separated by *ca*. 0.15 eV at the geometry of the anion, the separation between the $^2A_1$ and $^2B_2$ states is roughly an order of magnitude greater when reckoned from the respective diabatic minima. Also consistently predicted is that the minimum on the $^2B_2$ surface is *below* the lowest energy point on the C_{2v} subspace of the $^2A_1$ surface, with the two fourth-order parametrizations giving adiabatic separations of roughly 540 cm^{-1}. It should be pointed out that this ordering is opposite that associated with the positions of the zero-point levels of the two states, both as observed experimentally as well as calculated, an observation that will be revisited shortly. The $^2A_1$ state, all models predict, does not have an equilibrium geometry with C_{2v} symmetry; rather, the minimum energy C_{2v} structure has an imaginary frequency along a mode of b_2 symmetry (which, of course, couples the two electronic states) and there are consequently two equivalent minimum energy, and distorted, structures. However, the magnitude of the stabilization energy associated with this effect is very small (see Ref. [4] for a brief discussion and a graphical depiction); this energy difference is less than 5 cm^{-1} for both the AP2 and AP4 parametrizations which are the most accurate in these regions of the potential energy surfaces. Stabilization energies that accompany distortion of the $^2A_1$ state to C_s symmetry given by the vertical parametrizations differ substantially—and track with the magnitude of the imaginary frequency—VP2 and VP4 giving differences of 380 and 300 cm^{-1}, respectively. The LVC model fails dramatically in describing this area of the potential surface; specifically, it predicts that the $^2A_1$ geometry is the (only) transition state on the minimum energy path linking the two states (see Fig. 2). Unlike the better potentials (see Fig. 4 of Ref. [4] for the corresponding AP4 potential, which qualitatively resembles the ab initio result), which predict that there is a fairly appreciable pseudorotation barrier between the $^2A_1$ and $^2B_2$ regions of the surface, such a feature is absent from the LVC model, principally because it grossly underestimates the energy difference between the two states. Since the AP2 and AP4 models give the exact ab initio surface through quadratic terms at the $^2A_1$ stationary point, the rather large stabilization energies associated with the VP2 and VP4 models are unrealistic; they are an artifact associated with deterioration in the quality of the potential surfaces as one moves away from the anion geometry which serves as the basis for parametrization of the vertical methods.

Given the accurate reproduction of the experimental spectrum with a very slightly adjusted ab initio potential [4] (as well as the truly ab initio potential used here, as shown in the next subsection), it is not unlikely that the "dimple" in the adiabatic potential of the $^2A_1$ state is real in the sense that it reflects the actual (exact) adiabatic potential of this state. In other words, in the typical language of quantum chemistry, the ground[8] $\tilde{X}^2A_1$ state of HCO_2 might not "be C_{2v}". However, it most certainly is from the spectroscopic point of view, since the energy difference between the C_{2v}

[7] *Coupled-Cluster techniques for Computational Chemistry*, a quantum-chemical program package by J.F. Stanton, J. Gauss, M.E. Harding, P.G. Szalay with contributions from A.A. Auer, R.J. Bartlett, U. Benedikt, C. Berger, D.E. Bernholdt, Y.J. Bomble, L. Cheng, O. Christiansen, M. Heckert, O. Heun, C. Huber, T.-C. Jagau, D. Jonsson, J. Jusélius, K. Klein, W.J. Lauderdale, D.A. Matthews, T. Metzroth, D.P. O'Neill, D.R. Price, E. Prochnow, K. Ruud, F. Schiffmann, W. Schwalbach, S. Stopkowicz, A. Tajti, J. Vázquez, F. Wang, J.D. Watts and the integral packages MOLECULE (J. Almlöf and P.R. Taylor), PROPS (P.R. Taylor), ABACUS (T. Helgaker, H.J. Aa. Jensen, P. Jørgensen, and J. Olsen), and ECP routines by A. V. Mitin and C. van Wüllen. For the current version, see http://www.cfour.de.

[8] The $^2A_1$ state is the ground state because it has the lower zero-point vibronic level even though it does not represent the lowest state on the adiabatic surface.

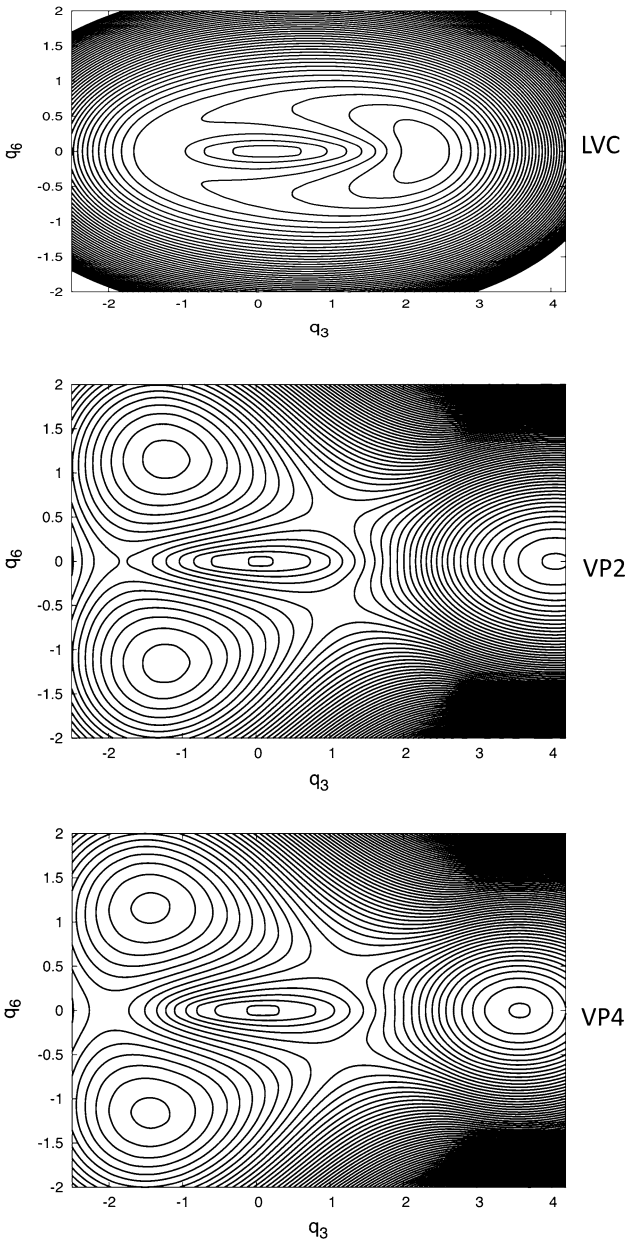

Fig. 2 Lower sheet of the adiabatic potential energy surface of HCO_2 with the various vertical parametrization approaches. At each coordinate point (q_3, q_6), the energy was minimized with respect to the other coordinates. Note that one can proceed monotonically downhill from the C_{2v} $^2A_1$ geometry (*left side of figure*) to the $^2B_2$ minimum (*right side*) on the LVC surface; in the others (as well as the AP2 and AP4 surfaces, which both qualitatively resemble the ab initio surface and Fig. 4 of Ref. [4]), the $^2A_1$ and $^2B_2$ regions are separated by appreciable pseudorotation barriers. Contours are drawn at 50 cm^{-1} intervals

and C_s minimum energy points is so small that the zero-point level is well above the former. Whether the exact adiabatic surface has a C_{2v} or C_s minimum is impossible to tell from either experiment or the present calculations, because there is no spectroscopic signature of the smooth and continuous change that occurs in the vibronic level positions with variation of the coupling strength (or gap) from "barely C_{2v}" to the qualitative (C_s) situation consistent with the present calculations. All that can be said is that the potential of the $^2A_1$ state is very flat with respect to asymmetric distortion. It should be noted that this departure from what might perhaps be expected behavior is *not* due to what is often termed "artifactual" symmetry breaking [33]; it is, instead, due to the pseudo-Jahn–Teller coupling that is represented by off-diagonal terms in the vibronic Hamiltonian used here. A similar "is it symmetric or not?" issue arises *vis-a-vis* the equilibrium geometry of the strongly coupled ground state of the NO_3 radical [6, 34].

Perhaps, more noteworthy is that the potential energy surface of the $^2A_1$ state is much more affected by the vibronic interaction than is that of the $^2B_2$ state which, by contrast, behaves like a rather rigid molecule with both b_2 frequencies in excess of 1,000 cm^{-1}. This, despite the fact that the vertical gaps between the two states at the $^2A_1$ and $^2B_2$ minima are of comparable magnitude. This phenomenon reflects the highly coordinate-dependent nature of the coupling between the two states; specifically, the linear coupling constant λ_6 at the vertical (anion) geometry (840 cm^{-1}) is very much different from that at the $^2A_1$ geometry (1,341 cm^{-1}) as well as the $^2B_2$ geometry (491 cm^{-1}), where λ_6 is about half that at the anion geometry. Thus, it is the coupling along q_6, which is primarily a wagging motion of the hydrogen atom, which is the driving force for the curiously different adiabatic potential energy surfaces along q_5 and q_6 for the two lowest-lying electronic states of HCO_2. The LVC model is inherently unable to account for the coordinate dependence of the coupling strength, which makes it entirely unsuitable for describing HCO_2. By contrast, the VP2 and VP4 methods both account for this important effect. The latter two methods perform somewhat unsatisfactorily for the C_s region of the potential (with respect to displacements of q_5 and q_6), mostly because they use the diabatic force constants F_{55} and F_{66} from the vertical geometry. There is a fairly substantial coordinate dependence in the magnitude of the F_{55} diabatic force constant that arises from the substantial difference in bond angle between the $^2A_1$ (144.8 degrees) and $^2B_2$ (112.5 degrees) electronic states.

At this juncture, a remark should be made about the ordering of the two lowest electronic states in HCO_2. The ab initio calculations suggest that the lowest point on the adibatic potential energy surface corresponds to the minimum of the $^2B_2$ electronic state, but the experimental evidence, supported by simulations of the spectrum, for a $^2A_1$ ground state is firm. The only way that such a situation can occur, of course, is if the zero-point energy of the $^2A_1$ state is substantially lower than that of the $^2B_2$ state. This

effect has primarily two sources; the CH bond in the $^2A_1$ state is a bit longer than in the $^2B_2$ state, with the result that the harmonic frequency of the CH stretching mode is about 800 cm^{-1} lower in the former. This accounts for 400 cm^{-1} of the difference of *ca.* 860 cm^{-1} that exists between the roughly 540 cm^{-1} difference between the adiabatic minima and the experimental splitting of 318 cm^{-1}. The remainder comes from the coupling modes, and the source of this effect comes, at least in part, from the substantially different vibronic coupling strengths that are operative in the two states. It is the $^2A_1$ state that experiences the stronger coupling, exhibiting a profoundly affected potential energy surface, and it is the $^2A_1$ state that is more stabilized by zero-point energy. Thus, vibronic coupling, while not manifested in a dramatic way in the laboratory spectrum, reveals itself in this perhaps subtle effect with a significant consequence: the reordering of electronic states. In addition, vibronic coupling is also the principal source of the quite profound bending anharmonicity found in HCO_2 (experimentally observed levels of v_3 and $2v_3$ in the $\tilde{X}^2A_1$ state are 564 and 1,086 cm^{-1}, compared to 570 and 1,058 cm^{-1} from the simulated spectrum) (see footnote 1).

The discussion above relates specifically to the areas around the minimum energy C_{2v} structures of the $\tilde{X}^2A_1$ and $\tilde{A}^2B_2$ electronic states of HCO_2, where the adiabatic parametrizations are designed to perform best. How do they do for the entire range of displacements that are relevant to the problem? A pictorial answer to this question, as it regards the totally symmetric coordinates q_1, q_2 and q_3, is provided

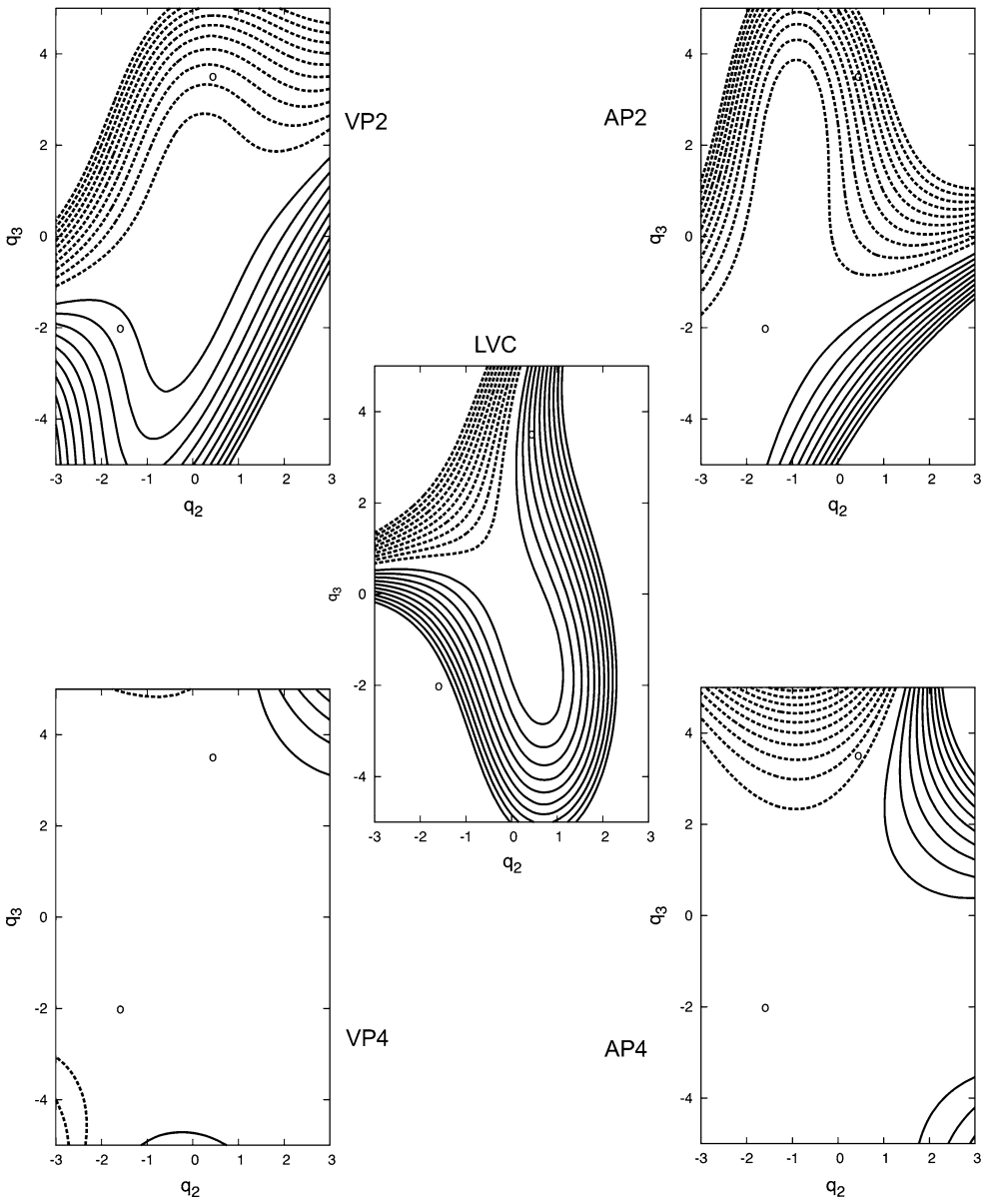

Fig. 3 Contour plot of the difference between the various model Hamiltonian $^2A_1$ adiabatic surfaces and the corresponding ab initio potential. The coordinates q_2 and q_3 are the symmetric CO stretch and OCO bending normal coordinates of the anion; the plot is a cut through the C_{2v} potential at $q_1 = 0$ (the CH stretch). Contours are drawn at intervals of 100 cm^{-1}; *solid contours* are associated with regions of the surface where $V_{\text{model}} < V_{ab\ initio}$; *dashed contours* are where the model potential is above the ab initio surface. The *small circles* represent the values of q_2 and q_3 at the $^2A_1$ and $^2B_2$ minimum energy geometries (see Table 1 for exact coordinates), and the *coordinate origin* corresponds to the geometry of the anion

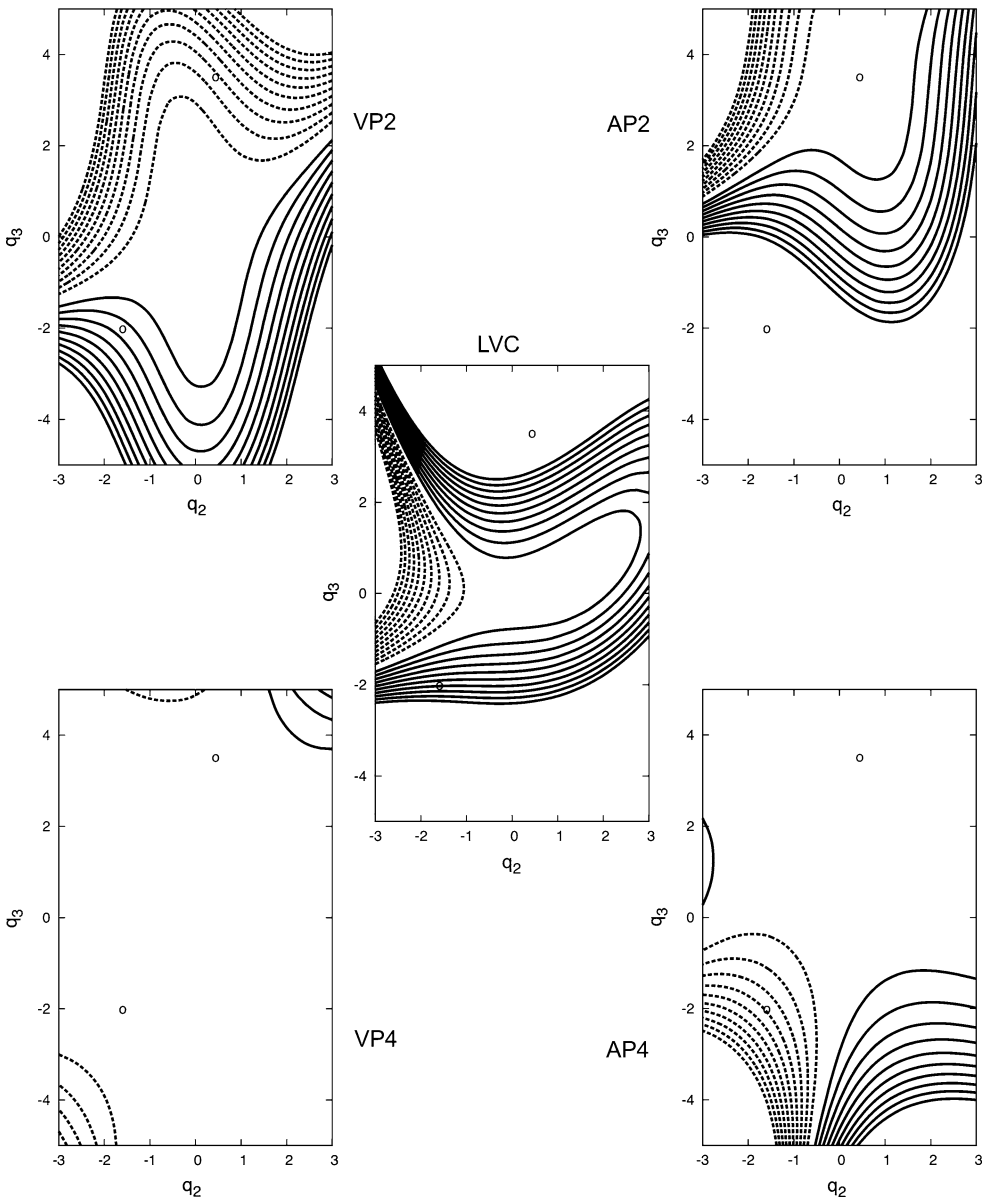

Fig. 4 Contour plot of the difference between the various model Hamiltonian $^2B_2$ adiabatic surfaces and the corresponding ab initio potential. See caption to Fig. 3 for further elaboration

by Figs. 3 and 4, which display the difference between ab initio and model Hamiltonian potential energy surfaces for both electronic states. For visualization purposes, these contour representations are cuts through the potential at $q_1 = 0$, which is the equilibrium value for the anion and is only slightly different from the neutral radical geometries (see Table 1). These two figures vividly illustrate the strengths and weaknesses of the various parametrization schemes. First, and owing to the substantial displacements upon electron detachment from the anion, the LVC model does very poorly in describing both surfaces near the equilibrium geometries of the neutral states; it is accurate only quite near the anion geometry. This, in addition to the fact that the model does not include the coordinate-dependent linear coupling that is essential to describe HCO_2 correctly, means that the LVC model is simply unsuitable for this molecule, where the geometry changes that occur upon photodetachment are significant.

For the quadratic VP2 and AP2 models, a much larger region of the potential is described very accurately (within $100\,\mathrm{cm}^{-1}$ of the ab initio result, which is the area within the first contour) than for the LVC model, with the regions around the anion and the neutral radical minima, respectively, treated most satisfactorily. While the AP2 potentials are clearly excellent near the associated minima around which they are parametrized, they do not do very well at the geometry of the other state. The overall behavior of the VP2 model, however, is not significantly better, despite the fact that the coordinate origin of this model (the anion geometry) is intermediate between the neutral state geometries.

However, when one goes to quartic terms in the diagonal blocks of the potential, the VP4 model faithfully reproduces the ab initio surface over the entire range spanned by the two minima, while the $^2A_1$ and $^2B_2$ surfaces associated with the AP4 models, although considerably better than AP2, still are not entirely satisfactory near the C_{2v} minimum energy structures of the other ($^2B_2$ and $^2A_1$, respectively) neutral state. Nevertheless, both quartic models provide very good reproductions of the ab initio surface.

Another aspect of the parametrization that is worthy of discussion is the treatment of conical intersections. In HCO_2, in which there is a significant energy gap between the two states at both the $^2B_2$ minimum, where the OCO bond angle is "small", and at the $^2A_1$ geometry, where the OCO bond angle is considerably greater, the surfaces necessarily cross at intermediate bond angles. One set of parameters that quantitatively describes this seam of conical intersections (in HCO_2, it is a two-dimensional surface) is the location and energy of the lowest energy point on the intersection seam. These coordinates and energies are given in Table 1 for all of the model Hamiltonians (see footnote 4), as well as the ab initio potential, where it can be seen that all parametrizations do a reasonable job of characterizing this important point on the potential energy surfaces. The VP2 and VP4 models are in essentially perfect agreement with the ab initio potential, due to the proximity of the conical intersection seam minimum to the anion geometry (where the VPn models perform best). Even the LVC model, woefully inadequate for so many aspects of this problem, fares reasonably well. Indeed, it gives a prediction for the seam minimum that is far superior to the AP2 model, which provides what is—by far—the poorest performance. From the excellent VP4 to the poorest AP2 result, the performance of the various parametrizations in this context is easily understood in terms of how the methods are defined and the general location of the intersection seam, which is displayed graphically in Fig. 5.

It needs to be emphasized that the comments and conclusions above are all based on the specific case of the $^2A_1$ and $^2B_2$ states of HCO_2. The salient features of this vibronic system are as follows:

1. The changes in geometry that accompany anion photodetachment are quite large for both the $^2A_1$ and $^2B_2$ states;
2. The difference between geometries of the two vibronically coupled states is also exceptionally large, with OCO bond angles differing more than thirty degrees;
3. At the respective minima on the potential energy surfaces, both states are relatively far apart, with separations of about 1 eV, and, conversely, less than 0.2 eV apart at the anion geometry;

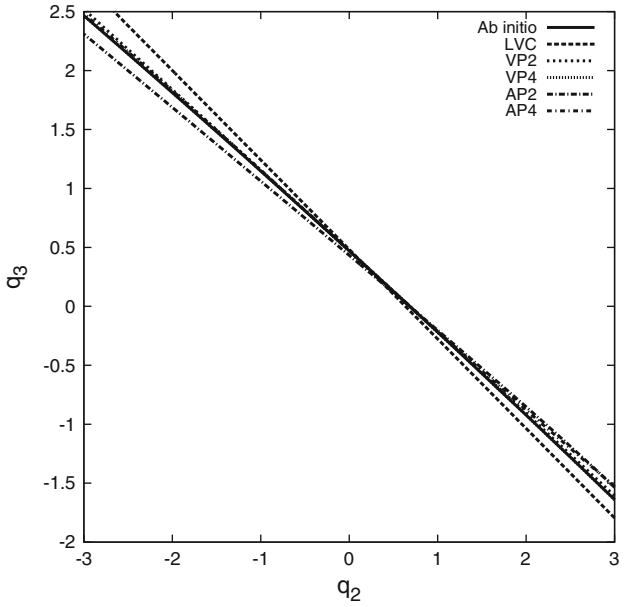

Fig. 5 Projection of the two-dimensional seam of conical intersections onto the $q_1 = 0$ plane, as governed by the ab initio and various model potential adiabatic potential energy surfaces. Note the proximity of the anion geometry to the conical intersection seam. See caption to Fig. 3 for a description of the coordinate system

4. The seam of conical intersections is close to the geometry of the anion and quite distant from the two minima, with the latter observation a simple consequence of 3) above;
5. The linear coupling strength between the two states is a very strong function of coordinates, especially for the CH wagging motion q_6. As a result, the vibronic coupling has a much greater effect on the potential surface of the $^2A_1$ state, despite the quite similar energetic vertical gaps that exist at the C_{2v} minimum energy geometries and the fact that coupling effects on the potential are given, to leading order, by Eq. (6).

It is *only when considerations like this are made* that one can objectively choose a "best" parametrization scheme for the KDC Hamiltonian. For HCO_2, consideration 5) demands that the LVC approximation of a global linear coupling strength be abandoned. Moreover, non-adiabatic effects in the spectroscopy of HCO_2 are actually not nearly so conspicuous as in systems such as NO_3 [34] or BNB [35]. Indeed, the SEVI spectra of HCO_2 and DCO_2 display only a few (and weak) features that are due to activity in non-symmetric b_2 vibrational levels. This, of course, is a consequence of 3) above, and means that the most important part of the KDC Hamiltonian in the present case is the description of Franck-Condon activity in totally symmetric modes, a requirement that strongly favors the adiabatic parametrization approach. If the non-adiabatic effects were more important, then it might be preferable to

go with VP4 since it describes the conical intersection region so well while still doing a serviceable job near the equilibrium geometries of the $^2A_1$ and $^2B_2$ states. But, of course, the above considerations apply only because the seam of intersections runs close to the coordinate origin. One alternative scenario that could be envisioned for another molecule would be one where the two neutral state geometries are close to one another, as well as the seam of conical intersections, but all relatively distant from the vertical geometry. In that case, the adiabatic parametrization would unquestionably be preferable. The choice of parametrization is clearly not a glibly transferable, black-and-white, decision that applies to all vibronically coupled systems; rather, it requires an analysis of the system at hand and an understanding of the important physics of the problem. The only thing that can be said is that, in the limit of small displacements from the absorbing state geometry, all of these methods are equivalent. It is only in cases like HCO_2, where profound geometry changes are observed, that dramatic differences will be found between results obtained with the various procedures. By contrast, the very simple LVC model does an excellent job with describing the negative ion photodetachment spectrum of the nitrate anion to the ground $\tilde{X}^2A_2'$ state of the NO_3 radical [6, 34, 36], where the geometry change is only very slight.

4.2 Simulated electron photodetachment spectra of HCO_2^-

The simulated spectra of HCO_2^- photodetachment are displayed in Figs. 6 and 7 and can be compared with the general features of the experimental spectrum shown in Fig. 8 along with that given by the AP4 parametrization. In general, the quality of the simulations reflects the degree to which the methods have succeeded in reproducing the high-quality ab initio potential energy surfaces. Specifically, the spectrum given by LVC—the one model that is too fundamentally constrained to be applicable to this

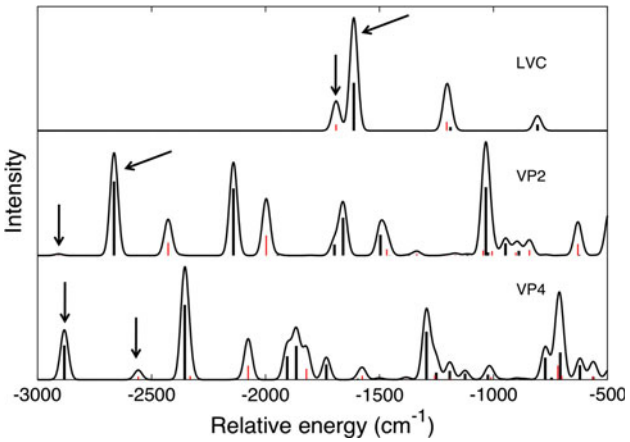

Fig. 6 Simulation of the negative ion photoelectron spectrum of HCO_2 using the three vertical parametrization schemes discussed in this work. The origins of the $^2A_1$ and $^2B_2$ electronic states of the neutral are shown by *arrows*; in all cases, the stronger of the two features represents the $^2A_1$ origin. The energy scale is relative to the zero-point corrected $^2A_1$ *diabatic* potential at the coordinate origin in all cases. States of $^2A_1$ and $^2B_2$ vibronic symmetries are designated by *black and red sticks*, respectively

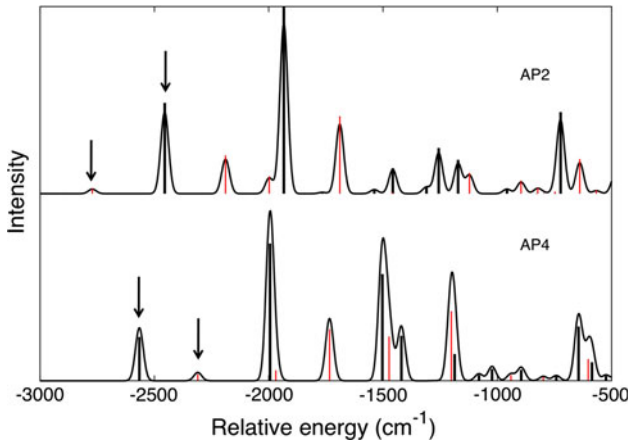

Fig. 7 Simulation of the negative ion photoelectron spectrum of HCO_2 using the two adiabatic parametrization schemes discussed in this work. The origins of the $^2A_1$ and $^2B_2$ electronic states of the neutral are shown by *arrows*; in all cases, the stronger of the two features represents the $^2A_1$ origin. The energy scale is relative to the zero-point corrected $^2A_1$ *diabatic* potential at the coordinate origin in all cases. States of $^2A_1$ and $^2B_2$ vibronic symmetries are designated by *black and red sticks*, respectively

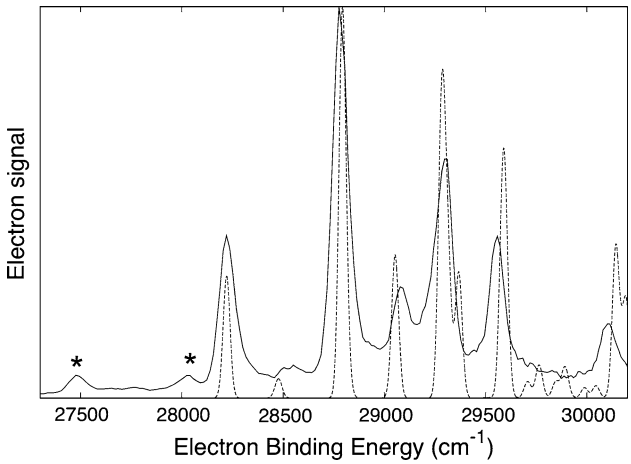

Fig. 8 Comparison of the SEVI spectrum of HCO_2 with the purely ab initio AP4 simulation, with the $^2A_1$ origin of the latter shifted to coincide with the experimental origin. The experimental features designated with an asterisk are those arising from vibrationally excited levels of the anion and were assigned in Ref. [4]. The intensities toward the higher end of the energy range shown, which is a region of near threshold detachment, are more severely affected by the Wigner threshold law, which is not taken into account in the simulations

difficult problem—bears very little resemblance to the experimental band profile. Indeed, apart from the fact that the LVC model, like all of the others studied here, predicts a small splitting between the respective origins of the $^2A_1$ and $^2B_2$ states with a substantially greater intensity of the former, the simulation would not be a very useful tool for assigning the experimental spectrum. This holds true even if one were to empirically shift the origins of the two states after correctly assigning the experimental features near 28,200 and 28,500 cm^{-1} (see Fig. 8) to the $^2A_1$ and $^2B_2$ origins, respectively. In particular, the intensities of the two 6_0^1 vibronic transitions predicted by the LVC model are so small that they are not visible in the simulated spectrum (see Table 1 and Fig. 5 in Ref. [4] for the assignments of the experimental photoelectron peaks to these transitions based on the AP4 simulation). This result is a direct consequence of a point that was emphasized in the preceding section: the importance of the coordinate dependence of the coupling strength in HCO_2 and the absence of this mechanism in the LVC parametrization.

Both the LVC and VP2 models lead to the incorrect prediction of a $^2B_2$ ground state in HCO_2. The spacings between the $^2B_2$ and $^2A_1$ origins ($E(^2B_2) - E(^2A_1)$, $-77\,cm^{-1}$ for LVC, -243 for VP2) differ substantially from the experimental result of $+318\,cm^{-1}$ and the qualitative finding that the $^2A_1$ state is lowest. In addition, relative to the more sophisticated parametrizations discussed below, the LVC overestimates the intensity of the $^2B_2$ origin, while VP2 underestimates it. It is not hard to see from Table 1 why this is so; the (very large) displacement along q_3 (the OCO bending mode) in the $^2B_2$ state is underestimated and overestimated by the two approaches, which in turn is reflected by concomitant shortcomings in predicting the associated Franck-Condon profiles. In the latter regard, the adiabatic parametrization approaches are to be preferred, since the displacements between the anion and the neutral states are fixed to the ab initio values in these models.

While the problem of predicting the relative strengths of the two origin transitions are absent from the AP2 spectrum, this method still makes a significant error in predicting their separation. In missing the experimental $^2A_1/^2B_2$ energy difference by some $635\,cm^{-1}$, a major shortcoming of the AP2 model is vividly apparent. Recall what aspects of the ab initio surface go into the adiabatic parametrization models: the force constants at the minimum energy C_{2v} geometries, the displacements along q_1, q_2 and q_3 which separate the final states from the anion geometry, and the vertical gap between the two states. Consequently, the adiabatic energy separation is not constrained by the model potential. To reproduce the ab initio value with fidelity, the parametrization—which is harmonic in the AP2 model—needs to accurately represent the energy reduction due to relaxation of the geometries from the anion to those of the final states. As can be seen from Table 1, the AP2 model underestimates the relaxation energy of the $^2A_1$ state and *substantially* overestimates that of the $^2B_2$ state. The consequence, of course, is that this particular parametrization gives a simulated spectrum in which the origin of the $^2B_2$ state is (erroneously) located well below that of the $^2A_1$ state. It is precisely the same phenomenon that gives rise to the similar error found in the VP2 spectrum. Both of these models, which neglect intrinsic anharmonicity (see footnote 1) in the totally symmetric modes, are unable to satisfactorily account for the energy differences that take place over the quite large coordinate displacements that occur for HCO_2. It is only with the quartic models—VP4 and AP4 discussed below—that the relaxation energies are accurately reproduced. Indeed, with both of these parametrizations, the relaxation energies are given to within $15\,cm^{-1}$ of their ab initio values.

The quality of the VP4 spectrum is very good. Unlike both the limited and harmonic LVC and VP2 treatments, this method correctly predicts that the $^2A_1$ origin is below that associated with the $^2B_2$ state. Not only that, but the magnitude of the separation derived from the VP4 KDC Hamiltonian ($327\,cm^{-1}$) is in very good agreement with the experiment separation of *ca.* $318\,cm^{-1}$. The rather faithful reproduction of the spectrum (compare with AP4 in Fig. 7 and the experimental profile in Fig. 8) with VP4 is not surprising, given how well this parametrization does in describing the adiabatic potential energy surfaces (see Figs. 3 and 4, as well as the previous subsection). Indeed, it is nearly as good as the AP4 spectrum and, in fact, gives a better adiabatic separation between the two origin bands. While the original theoretical work on this system [4] used only the AP4 treatment of the Hamiltonian, it is clear from the present work that the same assignments could have been made on the basis of a shifted VP4 simulation which, at least, has the advantage of having a more straightforward parametrization protocol.

An excellent reproduction of the SEVI spectrum is provided by the AP4 treatment. In this work, the AP4 calculation is strictly ab initio, while that used in Ref. [4] involved an empirical adjustment of the ab initio vertical gap of $+40\,cm^{-1}$ in order to roughly reproduce the separation of *ca.* $318\,cm^{-1}$ between the $^2A_1$ and $^2B_2$ origins. However, the present parametrization is, of course, that which was originally used to aid the assignment of the SEVI spectrum[9]; the *ex post facto* upwards adjustment of the gap was done simply to improve absolute agreement

[9] Apart from the different protocol used in this work to fix the quadratic diabatic constants of the coupling modes, which makes only a very slight difference when the AP4 approach is used.

with experimental band positions and of course was only possible when the assignment of the two origin features was clear. The overall agreement between the strictly ab initio AP4 calculation and the experimental spectrum, which can be best appreciated from Fig. 8, is quite remarkable. Simulations of this quality, which are likely almost always possible for systems of this type with the advanced parametrizations outlined in this work, are clearly useful aids for the assignment of the relatively high-resolution SEVI spectra, which can conspicuously reveal close-lying levels in vibronically coupled systems.

Acknowledgments This work is dedicated to Pekka Pyykkö, who has long taught us that molecules can be complicated things. Research presented here has been supported by the Deutsche Forschungsgemeinschaft (GA 370/5-1) and the Fonds der Chemischen Industrie (Mainz), by the US National Science Foundation, the US Department of Energy, and the Robert A. Welch Foundation (Grant F-1283) (Austin) and the Air Force Office of Scientific Research (Berkeley).

References

1. Ruscic B, Schwarz M, Berkowitz J (1989) J Chem Phys 91:6780
2. Kim EH, Bradforth SE, Arnold DW, Metz RB, Neumark DM (1995) J Chem Phys 103:7801
3. Neumark DM (2008) J Phys Chem A 112:13287
4. Garand E, Klein K, Stanton JF, Zhou J, Yacovitch TI, Neumark DM (2010) J Phys Chem A 114:1374
5. Köppel H, Domcke W, Cederbaum LS (1984) Adv Chem Phys 57:59
6. Stanton JF (2007) J Chem Phys 126:134309
7. Beckers H, Esser S, Metzroth T, Behnke M, Willner H, Gauss J, Hahn J (2006) Chem Eur J 12:832
8. Tew DP, Klopper W, Heckert M, Gauss J (2007) J Phys Chem A 111:11242
9. Müller H, Köppel H, Cederbaum LS (1994) J Chem Phys 101:10263
10. Raab A, Worth GA, Meyer H-D, Cederbaum LS (1999) J Chem Phys 110:936
11. Hazra A, Nooijen M (2005) J Chem Phys 122:204327
12. Neugebauer J, Baerends EJ, Nooijen M (2005) J Phys Chem A 109:1168
13. Stanton JF, Sattelmeyer KW, Gauss J, Allan M, Skalicky T, Bally T (2001) J Chem Phys 115:1
14. Cederbaum LS, Köppel H, Domcke W (1981) Int J Quantum Chem S 15:251
15. Zhu X, Yarkony DR (2009) J Chem Phys 130:234108
16. Iung C, Ribeiro F, Sibert EL III (2006) J Phys Chem A 110:5420
17. Haller E, Köppel H, Cederbaum LS (1985) J Mol Spectrosc 111:377
18. Viel A, Eisfeld W (2004) J Chem Phys 120:4603
19. Eisfeld W, Viel A (2005) J Chem Phys 122:204317
20. Mahapatra S, Cederbaum LS, Köppel H (1999) J Chem Phys 111:10452
21. Mahapatra S, Vallet V, Woywod C, Köppel H, Domcke W (2005) J Chem Phys 123:231103
22. Ichino T, Gianola AJ, Lineberger WC, Stanton JF (2006) J Chem Phys 125:084312
23. Raghavachari K, Trucks GW, Pople JA, Head-Gordon M (1989) Chem Phys Lett 157:479
24. Almlöf J, Taylor PR (1987) J Chem Phys 86:4070
25. Watts JD, Gauss J, Bartlett RJ (1992) Chem Phys Lett 200:1
26. Szalay PG, Gauss J, Stanton JF (1998) Theor Chim Acta 100:5
27. Ichino T, Gauss J, Stanton JF (2009) J Chem Phys 130:174105
28. Mattie R (1995) Ph.D. thesis, University of Florida
29. Stanton JF, Gauss J (1994) J Chem Phys 101:8938
30. Purvis GD III, Bartlett RJ (1982) J Chem Phys 76:1910
31. Dalgarno A, Stewart AL (1958) Proc Roy Soc London A 247:245
32. Dunning TH Jr (1970) J Chem Phys 53:2823
33. Davidson ER, Borden WT (1983) J Phys Chem 87:4783
34. Weaver A, Arnold DW, Bradforth SE, Neumark DM (1991) J Chem Phys 94:1740
35. Asmis KR, Taylor TR, Neumark DM (1999) J Chem Phys 111:8838
36. Mayer M, Cederbaum LS, Köppel H (1994) J Chem Phys 100:899